

Electrohydrodynamic Propulsion for Miniature Ships

Felix M. Moesner, Philipp S. Bühler, Diego C. Politano and Paolo V. Prati

Swiss Federal Institute of Technology Zurich (ETHZ) • Institute of Robotics
ETH Center, 8092 Zurich, Switzerland

Fax: +41 1 632 1078 • Email: moesner@ifr.mavt.ethz.ch • WWW: <http://www.ifr.mavt.ethz.ch>

ABSTRACT

Pumps utilizing electric traveling waves as the conveyor of liquids have already been presented in various publications. In those considerations, a dielectric liquid has been chosen as the media to propel. Inversely, it is conceivable to use pumps as propulsion motors for tiny vessels.

Hereinafter, the proposed electrohydrodynamic (EHD) propulsion motor is based on the electric tube device which has been introduced in earlier papers by the first author for the task of particle mass transportation [1,2]. The device is made by winding 6 parallel and insulated wires to a cylindrical tube. In the present work, the employed wires have a diameter in the range of $56 \mu\text{m} \sim 236 \mu\text{m}$. Upon the application of multi-phase voltages to the monolayer-electrodes, the created traveling electric field wave carries the charged liquid in the same direction.

Various EHD propulsion motors have been fabricated and optimized through a series of experiments. Optimizing parameters involve electrode-dimensions, fabrication materials, applied voltages and frequencies. As evaluative parameters, the propulsion pressure and the rate of liquid flow is determined. Constant and precise liquid propulsion is achieved. It is further shown that this tube structure has a high potential for miniaturization.

Keywords: electrohydrodynamic, propulsion, miniature ship, flow rate, pressure, charge relaxation time

I. INTRODUCTION

Miniaturization in many fields has an increasing importance in our modern technological world. In this sense, the demand is raising for new kinds of propulsion motors which fit into a microscaled domain. In this paper, a propulsion motor for a future tiny vessel is presented. The vessel, which will be either a miniature ship or a submarine of maximal a few centimeter length, is intended to incorporate both the autonomous navigation by a microprocessor and the powering of the propulsion. Previously, the problem to find a suitable propulsion motor ready to be mounted to the vessel has to be solved.

The focus of this paper lies on the application of electric traveling fields for the propulsion task. Originally, it is not a new idea to use electric fields to move a liquid media. In the sixties, some theoretical models of pumps have been published. Pickard and Stuetzer have proposed a model for an induction-type electrohydrodynamic (EHD) pump [3,4] which has

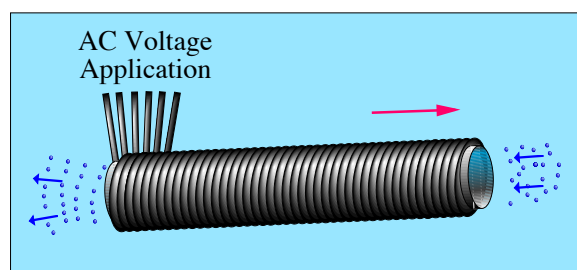


Fig. 1: Schematic of an EHD propulsion motor.

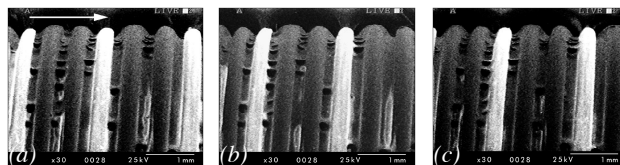


Fig. 2: Series of dynamic SEM micrographs showing quantitative negative charge (white) progressing in sync with a three-phase traveling wave on the outside surface of the propulsion motor.

been studied by Melcher in further details [5,6,7]. Pumps have also been constructed and tested. In all those cases, large pumps have been designed that function with very high voltages and transport solely insulator-fluids. In recent time, researchers began to built small-scaled pumps [8].

The EHD propulsion motor introduced in this paper is based on the same principle; i.e. inversely, a pump also functions for propulsion purposes. Currently, it produces its utmost performance in dielectric liquid revealing some interesting properties. The design itself comprises of structural simplicity. If we consider that the employed method with the traveling electric wave is a surface effect, the EHD motor has a very interesting miniaturization potential when compared to a conventional motor following a volume effect. Furthermore, this EHD propulsion motor has no moving mechanical parts resulting in no wear and also permitting minimal heat-dissipation – a property indispensable for many applications.

II. PRINCIPLE OF EHD PROPULSION

The EHD propulsion motor consists of coiled up insulated monolayer electrodes connected to a multi-phase voltage source as shown in the schematic of Figure 1. Upon the application of the phase voltages, an electric field is created around the electrodes. The voltages are supplied in a time-varying manner, producing a traveling electric field. The progression of the traveling electric field can be shown indirectly by a series of scanning electron microscope (SEM) pictures, as presented in Figure 2 for the three-phase voltage application case. The electric wave and its surface charge distribution is traveling stepwise from left (a) to right (c). The white area represents negative surface charge.

During operation, the motor is immersed into a dielectric liquid which becomes polarized by the non-uniform electric field and receives a volume charge density corresponding the negative divergence of the polarization. Consequently, the charge is induced into the liquid due to the polarization. The charges interact with the traveling electric field so that the liquid and the charge are moving in direct relation. Figure 3 illustrates the propulsion mechanism. Step a: Polarization of the liquid takes place around the electrodes. Charges get induced into the liquid. Step b: The electric field proceeds to the next electrode pulling the charged liquid in sync. Step c: The liquid becomes repolarized around the electrodes. More and more charges are induced into the liquid. Step d: Again, the electric wave is moving to the next electrode dragging the charged liquid in sync.

An estimation for the appropriate frequency of the applied voltages is given by the charge relaxation time τ [s].

$$\tau = \epsilon / \sigma \quad (1)$$

It is the ratio of the dielectric constant ϵ [C/Vm] to the elec-

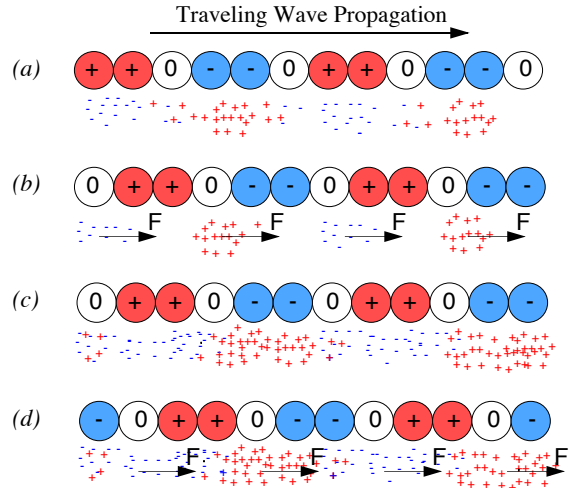


Fig. 3: Principle of the EHD propulsion motor. The liquid around the electrodes becomes charged and is transported in sync with the traveling electric field.

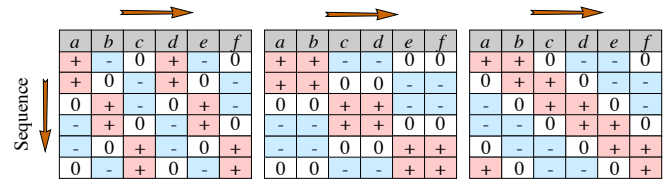


Fig. 4: Three-phase (a), double three-phase (b) and six-phase (c) activation sequences.

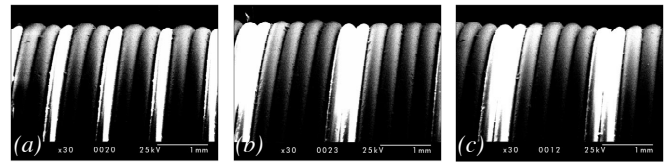


Fig. 5: Surface charge distribution in three-phase (a), double three-phase (b) and six-phase (c) activation mode.

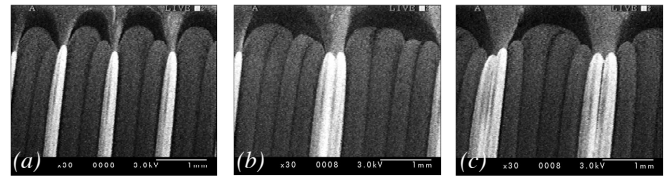


Fig. 6: Same as above. The SEM acceleration voltage is lowered to 3 kV, resulting in distorted images.

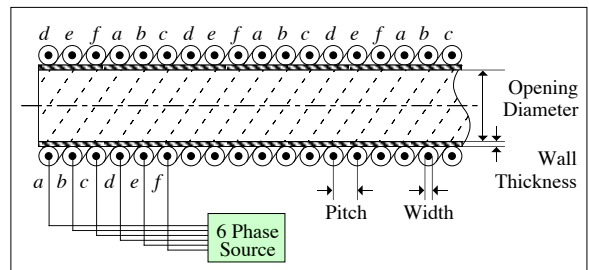


Fig. 7: Cross-section of the EHD propulsion motor illustrating its structure and its six-phase voltage supply attachments.

trical conductivity σ [$1/\Omega\text{m}$] of the liquid. The smaller the ratio, the faster the charge relaxes. The polarization \mathbf{P} [C/m^2] of a dielectric liquid which is exposed to an electric field \mathbf{E} [V/m] amounts to

$$\mathbf{P}(x, y, z) = \epsilon \cdot \chi \cdot \mathbf{E}(x, y, z) \quad (2)$$

where χ is the scalar electric susceptibility of the liquid. At steady state the induced charge density is described by

$$\rho_0 = -\nabla \cdot \mathbf{P}(x, y, z) \quad (3)$$

and the instantaneous charge density is expressed by

$$\rho(x, y, z, t) = \rho_0 \cdot (1 - e^{-t/\tau}) \quad (4)$$

where τ is the charge relaxation time.

The charge ρ is pulled by the advancing traveling electric field \mathbf{E} generating a force density \mathbf{F} related to the Coulomb force. The produced force is formulated by (5).

$$\mathbf{F}(x, y, z) = \rho \cdot \mathbf{E}(x, y, z) \quad (5)$$

Since both ρ and \mathbf{E} are linearly dependent on the applied voltage V , the following relation can be written

$$F \propto V^2 \quad (6)$$

Among the applied multi-phase voltages, the three-phase, the double three-phase and the six-phase activation sequences, which are shown in Figure 4, have been chosen. The corresponding SEM images are presented in Figure 5 and 6. The latter pictures help to distinguish between the actual applied voltages to the single electrodes.

III. FABRICATION

The main advantage of the tube shape structure is the simple fabrication of the EHD propulsion motor. Polyimide enameled copper wires are spirally wound up in a monolayer onto a cylindrical substrate, fixed by a bond and finally removed from the substrate. Table 1 contains all fabricated EHD motors with information on electrode width/pitch and type of fixation bond.

TABLE I:
EMPLOYED BONDING MATERIALS AND WIRE DIAMETERS

Electrode Width/ Bond	56/63 μm	132/145 μm	190/200 μm	236/250 μm
Cyanoacrylate	✓	✓	✓	✓
Epoxy		✓	✓	✓
Urethane Spray			✓	✓
Adhesive Tape				✓

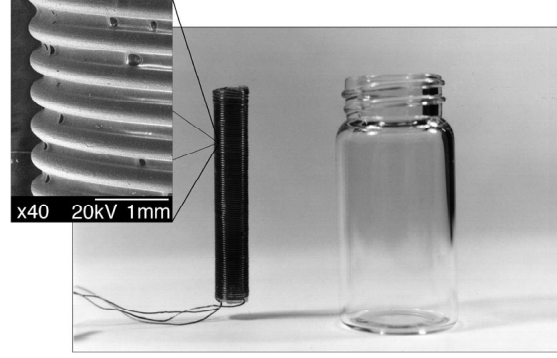


Fig. 8: EHD propulsion motor positioned upright next to a specimen container.

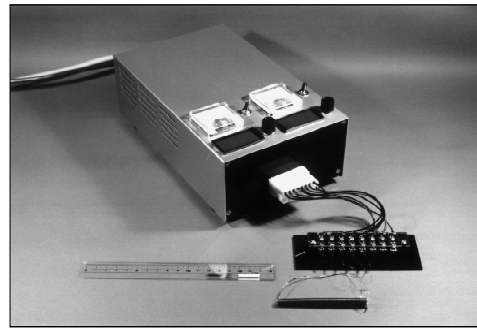


Fig. 9: The EHD propulsion motor is attached to the PC controlled voltage source via a connection bridge.

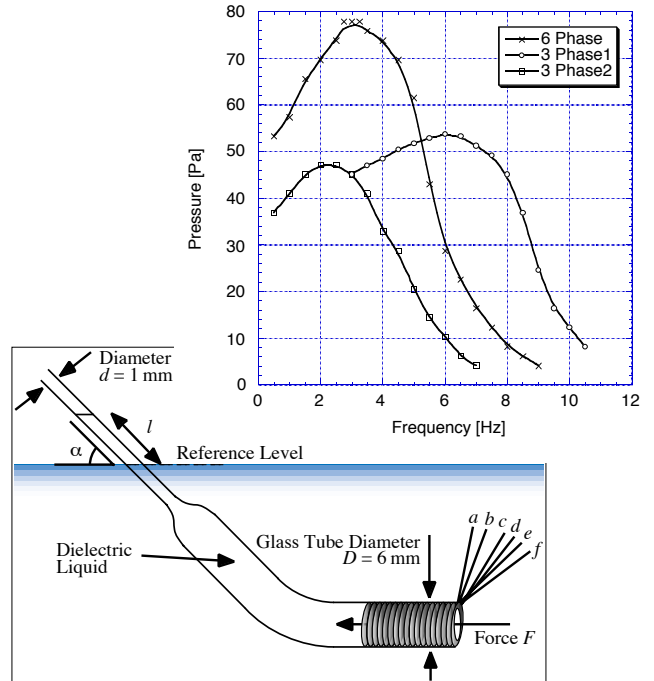


Fig. 10: Propulsion liquid pressure vs. applied frequency for the multi-phase case of a 132 μm pitched, epoxy bonded motor. The schematic shows the setup used for measuring the propulsion pressure.

Figure 7 shows the cross-section of the EHD propulsion motor. Among the fixation bonds, the adhesive tape proofed to be impracticable through its self-dissolving character when immersed into the liquid. The fixation with urethane spray produced a structure with insufficient robustness. The usage of either the cyanoacrylate or the epoxy compound resulted in practicable devices whose sample is depicted in Figure 8. The complete system including the programmable 16-channel voltage source is shown in Figure 9.

IV. PROPULSION PRESSURE

In a first experiment to evaluate the performance of the EHD propulsion motor, the liquid propulsion pressure is determined. The motor is inserted into a curved glass tube as shown in Figure 10 and immersed into the liquid (sunflower oil). The internal space of the motor is filled with a concentric solid cylinder leaving enough space for the liquid to pass. The produced pressure p [Pa] is calculated as

$$p = \sin \alpha \cdot l \cdot \rho_{liquid} \cdot g \quad (7)$$

where α is the incline angle of the glass tube, l is the climbing distance [m] of the liquid, ρ_{liquid} is the density [kg/m^3] of the liquid and g is the gravitational acceleration [9.8 m/s^2]. The measurement results are presented in the graphs of Figure 10 and 11. As expected, the six-phase voltage application produces the greatest propulsion effectiveness as shown in Figure 10. Furthermore it is stated, that the generated pressure is in clear relation to the applied voltage amplitude and to the frequency as shown in Figure 11. It is assumed that both the six-phase voltage application and the high voltage amplitude generate traveling electric fields with a greater effective penetration depth into the liquid. Thus, a higher propulsion pressure could have been achieved. Future theoretical considerations are needed to verify these experimental findings.

Figure 12 shows the pressure saturation curve of the propulsion motor dependent on the applied voltage. At low voltages up to 500 V amplitude, the pressure is proportional to the square of the voltage amplitude as previously expressed in equation (6). It is assumed that at higher voltage levels, a nonlinear behavior of the liquid limits the maximal pressure. Therefore, the pressure performance of the motor goes into saturation at a level of about 180 Pa.

V. RATE OF LIQUID FLOW

The liquid flow rate of the motor is measured in a straight glass tube. A marker object helps to evaluate the liquid velocity v_{Media} as illustrated in Figure 13. The flow rate Q [m^3/s] is described in equation (8).

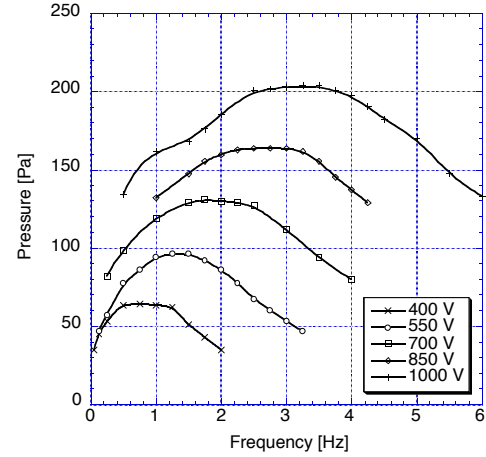


Fig. 11: Propulsion liquid pressure vs. applied frequency for a set of voltage amplitudes applied to a $190 \mu\text{m}$ pitched, epoxy bonded EHD motor.

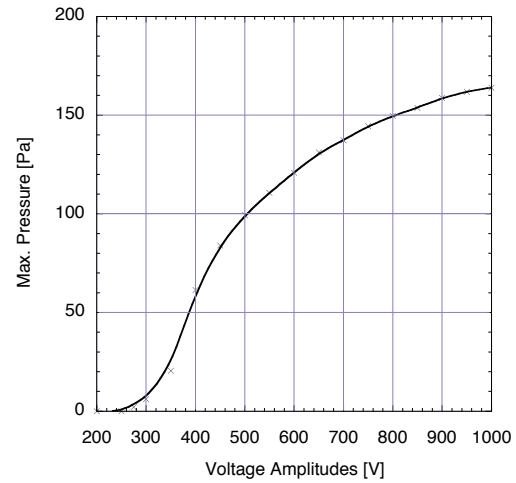


Fig. 12: Maximal pressure vs. amplitude of applied six-phase voltages to a $190 \mu\text{m}$ pitched, cyanoacrylate bonded motor. The frequency was set to 2 Hz. At higher voltage amplitudes, the pressure level shows a saturation.

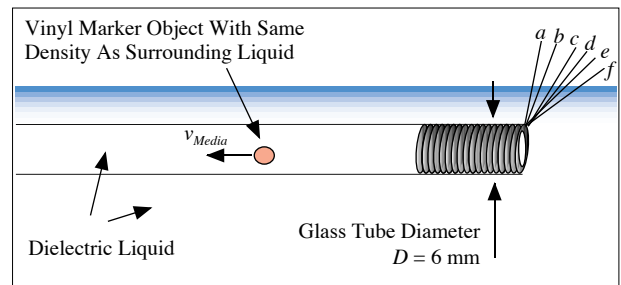


Fig. 13: Schematic of setup used for measuring the rate of liquid flow. A marker object helps to indicate the liquid flow velocity.

$$Q = v_{Media} \cdot (D/2)^2 \cdot \pi \quad (8)$$

The six-phase traveling wave propagation velocity is calculated by

$$v_{Field} = 6 \cdot pitch \cdot f \quad (9)$$

The measurements in the graph of Figure 14 reveal a constant liquid propulsion at different frequencies for various motor types. For all three cases, a voltage amplitude of 800 V is supplied to the electrodes.

The experimental results for a 250 μm pitched motor are presented in Figure 15 revealing the liquid velocity with a peak at 1.2 mm/s and the ratio of flow velocity to wave propagation velocity with a peak in the order of the relaxation time $\tau = 4.13$ s for sunflower oil where $\epsilon_r = 3.16$ and $\sigma = 6.78 \cdot 10^{-14}$ (Ωm)⁻¹.

VI. CONCLUSION

The best performance has been achieved for a 190 μm pitched, epoxy bonded motor. A max. pressure of 205 Pa is reached with six-phase voltage application at 1 kV amplitude and at a frequency of 3.5 Hz. The max. flow rate is 31.5 $\mu\text{l}/\text{sec}$ at 0.8 kV amplitude and at 3 Hz. The propulsion proved to be very constant. Substantial performance improvement can be attained by a concatenation of concentric EHD propulsion motors.

ACKNOWLEDGMENTS

We wish to acknowledge the valuable collaboration of our colleagues S. Egawa, A. Fujita, and T. Niino. Highest appreciation is given to Professor T. Higuchi and to the Kanagawa Academy of Science & Technology, Japan.

REFERENCES

1. **Moesner**, F.M., and **Higuchi**, T., "Devices for Particle Handling by an AC Electric Field," *Proceedings IEEE Micro Electro Mechanical Systems*, Amsterdam, The Netherlands, January 1995, pp. 66-71.
2. **Moesner**, F.M., "Transportation and Manipulation of Particles by an AC Electric Field," *Doctoral Thesis ETH No.11961*, Swiss Federal Institute of Technology, Zurich, 1996.
3. **Pickard**, W.F., "Ion-Drag Pumping In Theory," *Journal of Applied Physics*, Vol. 34, 1963, pp. 136-146.
4. **Stuetzer**, O.M., "Ion-Drag Pumps," *Journal of Applied Physics*, Vol. 34, 1963, pp. 136-146.
5. **Melcher**, J.R., "Traveling-Wave Induced Electroconvection," *Physics of Fluids*, Vol. 9, No. 8, 1966, pp. 1548-1555.
6. **Melcher**, J.R., "Traveling-Wave Bulk Electroconvection Induced across a Temperature Gradient," *Physics of Fluids*, Vol.10, No6,1967, pp. 1178-1185.
7. **Melcher**, J.R., "Electric Fields and Forces in Semi-Insulating Liquids," *Journal of Applied Physics*, Vol. 2, 1976, pp. 121-132.
8. **Choi**, J.W., and **Kim**, Y.K., "Micro Electrohydrodynamic Pump Driven by Traveling Electric Fields," 30th IAS Annual Meeting Conference Record, 1995, pp. 1480-1484.

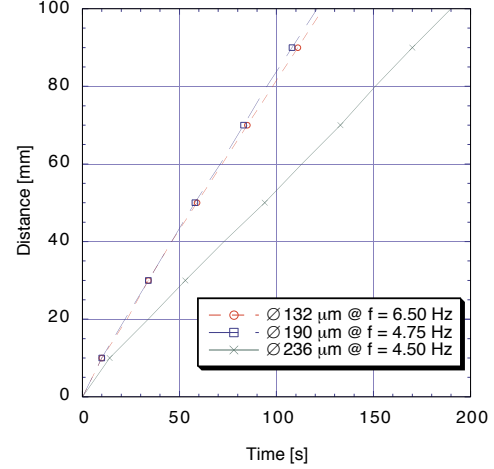


Fig. 14: Liquid flow distance vs. time measured at an applied voltage amplitude of 800 V. A very constant liquid propulsion is achieved.

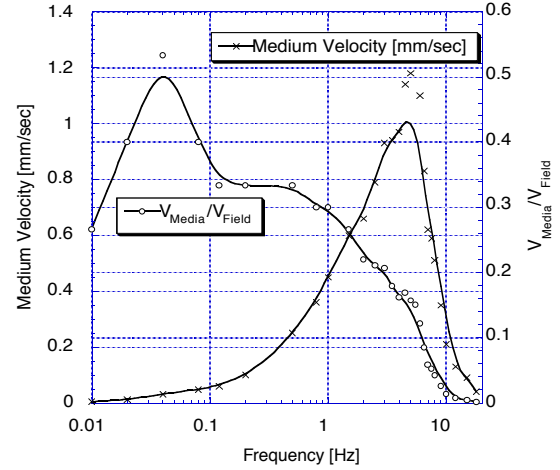


Fig. 15: Liquid velocity and ratio of flow velocity to wave propagation velocity vs. applied frequency. An amplitude of 1 kV is applied to 250 μm pitched electrodes.

PROCEEDINGS OF SPIE



SPIE—The International Society for Optical Engineering

Microrobotics and Microsystem Fabrication

Armin Sulzmann
Chair/Editor

16–17 October 1997
Pittsburgh, Pennsylvania

Sponsored and Published by
SPIE—The International Society for Optical Engineering

Cooperating Organizations
NIST—National Institute of Standards and Technology
CIMS—Coalition for Intelligent Manufacturing Systems
A-CIMS—Academic Coalition for Intelligent Manufacturing Systems



Volume 3202

SPIE is an international technical society dedicated to advancing engineering and scientific applications of optical, photonic, imaging, electronic, and optoelectronic technologies.